Electronic Materials Letters, Vol. 5, No. 1 (2009), pp. 23-27
DOI: 10.3365/eml.2009.03.023

Structural and Electrical Properties of (1-x)$Bi_5Nb_3O_{15}$-$x$$Bi_4Ti_3O_{12}$ Ceramics and 0.96$Bi_5Nb_3O_{15}$-0.04$Bi_4Ti_3O_{12}$ Thin Films Grown by Pulsed Laser Deposition

Myung-Eun Song, Tae-Geun Seong, Jin-Seong Kim, Kyung-Hoon Cho, Jong-Woo Sun, and Sahn Nahm*

Department of Materials Science and Engineering, Korea University,
1-5ga, Anam-dong, Sungbuk-gu, Seoul 136-701, Korea

A 0.96$Bi_5Nb_3O_{15}$-0.04$Bi_4Ti_3O_{12}$ (0.96B_5N_3-0.04B_4T_3) ceramic showed a high dielectric constant (k) of 314, probably due to the increased dipole moment caused by the replacement of Nb^{5+} ions by Ti^{4+} ions. The 0.96B_5N_3-0.04B_4T_3 films were well formed on the Pt/Ti/SiO_2/Si substrate. Films grown at temperatures lower than 400°C had an amorphous phase but small Bi_3NbO_7 crystals were considered to have been formed in these films. The film grown at 300°C exhibited a high k value of 83 with a low dielectric loss of 0.5%. The leakage current density of the film grown at low oxygen pressure (OP) was high and decreased with increasing OP to a minimum at an OP of 200 mTorr, after which it increased with further increase in OP. This variation of the leakage current density with OP was explained by the existence of oxygen vacancies and interstitial oxygen ions in the film. The 0.96B_5N_3-0.04B_4T_3 film grown under 200 mTorr OP exhibited a high k value of 83, a low leakage current density of 8×10^{-8} A/cm^2 at 0.3 MV/cm and a high breakdown field of 0.4 MV/cm.

Keywords: 0.96$Bi_5Nb_3O_{15}$-0.04$Bi_4Ti_3O_{12}$ film, low process temperature, dielectric constant, oxygen pressure

1. INTRODUCTION

Research has expanded on the dielectric thin films with high dielectric constant (k) that can be fabricated at temperatures lower than 400°C for application to thin film capacitors requiring a low processing temperature. The radio frequency (RF) or analog/mixed metal-insulator-metal (MIM) capacitors employed in semiconductor devices require low processing temperatures, due to the limitation of the VLSI back-end line integration temperature (< 400°C).[1] The embedded capacitor, which is formed inside printed circuit boards (PCBs) for the miniaturization of electronic devices, requires a low growth temperature (≤ 300°C).[2] The gate insulators of thin film transistors for organic light emitting diodes (OLEDs) on plastic substrates also need dielectric thin films with low processing temperatures. All dielectric capacitors fabricated at low temperature need a high k in order to obtain the necessary high capacitance. Amorphous TaTiO, $TiSiO_4$, $SrTiO_3$ and Pr_2O_3 dielectric films have been reported for RF or analog/mixed MIM capacitors but their k values were unsatisfactory.[3-6] Ba(Zr,Ti)O_3 (k = 17.3) and Ta_2O_5 (k = 21~25) films grown at room temperature were used for the gate insulators of OLEDs,[7-9] but their k value was relatively low. Ca-doped Pb(Zr,Ti)O_3 films with a high capacitance density were successfully grown on a copper substrate, but their processing temperature was too high for application to embedded capacitors in PCBs.[10,11] Therefore, a new, high k dielectric thin film which can be fabricated at low temperatures needs to be developed.

Recently, Bi-based, dielectric thin films such as $Bi_6Ti_5TeO_{22}$,[12] $Bi_{1.5}Zn_{1.0}Nb_{1.5}O_7$,[13-15] $Bi_2Mg_{2/3}Nb_{4/3}O_7$[16] and $Bi_5Nb_3O_{15}$[17,18] (B_5N_3) have been widely studied because of their high k values with low deposition temperatures. In particular, B_5N_3 films grown at 200 to 300°C using sputtering showed a high k value of 70, indicating that the B_5N_3 film is a good candidate material for thin film capacitors which require a low process temperature with a high k value.[17,18] Moreover, Mn-doping increased the k value of the B_5N_3 films with a improvement in electrical properties. Therefore, it was considered that the k value of the B_5N_3 film could be further increased when a proper amount of Nb^{5+} ions in the B_5N_3 film were replaced by Ti^{4+} ions because the Ti^{4+} ion is lighter and smaller than the Nb^{5+} ion and thus more easily deviated from its position under the electric field, thereby producing a large dipole moment. In this work, therefore, Ti-doped B_5N_3 films were formed and their structural and electrical properties were investigated for the first time to evaluate their potential as a thin capacitor requiring a low process temperature with a high k value. Furthermore, in order to find the optimum amount of Ti ions for the B_5N_3 film, the (1-x)$Bi_5Nb_3O_{15}$-$x$$Bi_4Ti_3O_{12}$ [(1-x)B_5N_3-xB_4T_3] ceramics with $0.0 \le x \le 0.3$

*Corresponding author: snahm@korea.ac.kr

were formed and their structural and dielectric properties were also studied in this work.

2. EXPERIMENTAL PROCEDURE

For the synthesis of (1-x)B_5N_3-$x$$B_4T_3$ ceramics with $0.0 \leq x \leq 0.3$, Bi_2O_3, Nb_2O_5 and TiO_2 (High Purity Chemicals, Japan) powders were ball-milled in a nylon jar with zirconia balls for 24 h. After drying, the mixed (1-x)B_5N_3-$x$$B_4T_3$ powders were fired at various temperatures for 10 h. The powders were subsequently ball-milled again for 48 h and dried, after which the hydraulically pressed pellets were sintered at 1150°C for 2 h. The 0.96B_5N_3-0.04B_4T_3 films were grown at various temperatures from 300 to 600°C on a Pt/Ti/SiO_2/Si(100) substrate using pulsed laser deposition (PLD). A Nd-YAG laser beam (NL303HT, EKSPLA, Lithuania) with a wavelength of 266 nm (the fourth harmonic generation), a repetition rate of 5 Hz and an energy fluency of 2 J/cm^2 was focused on the sintered 0.96B_5N_3-0.04B_4T_3 ceramic target rotating in a vacuum chamber under an oxygen pressure (OP) of 100 to 600 mTorr. The film structure was examined by scanning electron microscopy (SEM: Hitachi S-4300, Japan), atomic force microscopy (AFM: JSPM-5200, JEOL LTD., Japan) and X-ray diffraction (XRD: Rigaku D/max-RC, Japan). To measure the electric properties, Pt was deposited on the 0.96B_5N_3-0.04B_4T_3 film using conventional DC sputtering to form the top electrode of the MIM capacitor. The top electrode was patterned using a shadow mask to form a 380 μm-diameter disk. The capacitance and dissipation factor were measured by a precision LCR meter (Agilent 4285A, USA). The leakage current was measured using a programmable electrometer (Keithley 617, USA).

3. RESULTS AND DISCUSSION

Figure 1 shows the XRD patterns of the (1-x)B_5N_3-$x$$B_4T_3$ ceramicss with $0.0 \leq x \leq 0.3$ fired at 1100°C for 10 h. The peaks for the B_5N_3 phase, indicated by the full circles, were observed for the specimens with $x \leq 0.03$, implying that a small amount of the Ti ions was accommodated in the Nb site of the B_5N_3 phase. However, for the specimen with $x = 0.04$, the peak for the $Bi_3(NbTi)O_9$ phase started to be formed, while two phases, B_5N_3 and $Bi_3(NbTi)O_9$, coexisted for the specimens with $0.04 \leq x \leq 0.1$, and peaks for the $Bi_3(NbTi)O_9$ phase were only found when x exceeded 0.1. To elucidate the formation process of the $Bi_3(NbTi)O_9$ phase, the 0.94B_5N_3-0.06B_4T_3 specimen was fired at various temperatures, as shown in Figs. 2(a), (b), (c), and (d). For the specimen fired at 500°C, peaks for the Bi_3NbO_7 (B_3N) phase, indicated by the open circles, were observed along with those of the Bi_2O_3 and Nb_2O_5 phases, as shown in Fig. 2(a). Therefore, some of the Nb_2O_5 and Bi_2O_3 were considered to

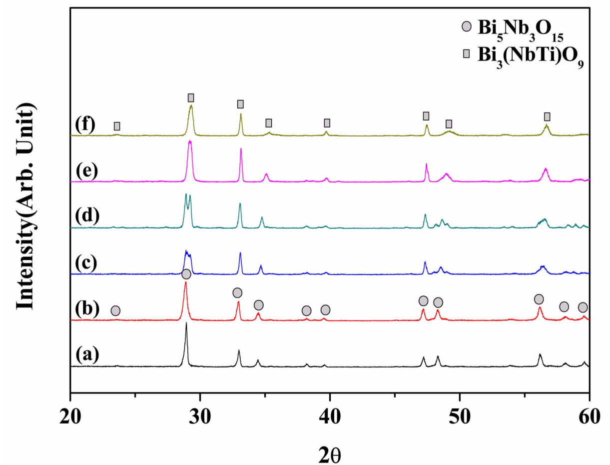

Fig. 1. XRD patterns of the (1-x)B_5N_3-xB_4T_3 specimens with $0.0 \leq x \leq 0.3$ fired at 1100 for 10 h: (a) x = 0.0, (b) x = 0.02, (c) x = 0.04, (d) x = 0.1, (e) x = 0.2 and (f) x = 0.3.

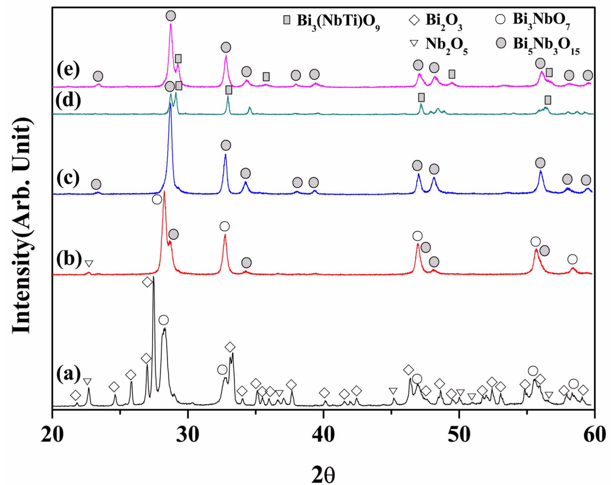

Fig. 2. XRD patterns of the 0.94B_5N_3-0.06B_4T_3 specimen fired at (a) 500°C, (b) 600°C, (c) 700°C, (d) 1100°C for 10 h, and (e) of the 0.8B_5N_3-0.2B_4T_3 ceramic fired at 700°C for 10 h.

have reacted at around 500°C to form the B_3N phase. As the firing temperature increased to 600°C, the B_5N_3 phase, indicated by the full circles was newly formed and the homogeneous B_5N_3 phase was found in the specimen fired at 700°C, as shown in Fig. 2(c). However, the $Bi_3(NbTi)O_9$ phase started to form when the specimen was fired at 1100°C and its amount increased with increasing firing temperature. Moreover, for the 0.8B_5N_3-0.2B_4T_3 specimen firing at 1100°C, only peaks for the $Bi_3(NbTi)O_9$ phase were observed, as shown in Fig. 1(e), but when this specimen was fired at 700°C, the major phase developed in this specimen was the B_5N_3 phase with a small amount of the $Bi_3(NbTi)O_9$ phase, as shown in Fig. 2(e). Therefore, the B_3N phase was considered to be a low temperature phase and the $Bi_3(NbTi)O_9$ phase was considered to have formed in the specimens containing a large

amount of Ti ions, as well as in the specimen fired at high temperature.

Figure 3 shows the k value of the (1-x)B_5N_3-$x$$B_4T_3$ ceramics with $0.0 \leq x \leq 0.3$ sintered at 1150°C for 2 h. The k value of the B_5N_3 ceramic of about 240 was similar to that of the specimen reported in the previous work.[19] It considerably increased with increasing x to a maximum value of 314 for the specimen with $x = 0.04$. Since the Ti^{4+} ions were incorporated into the Nb^{5+} sites for the specimens with $0.1 \leq x \leq 0.04$ and these Ti^{+4} ions are small and light compared to the Nb^{5+} ion, they were more easily deviated from their equilibrium position under an electric field, thereby increasing the dipole moment of the specimen. Therefore, the replacement of the Nb^{5+} ion by the Ti^{4+} ion was considered to have increased the k value of the specimens with a small amount of Ti ions. However, when x exceeded 0.04, it decreased, probably due to the formation of the $Bi_3(NbTi)O_9$ phase because the k value of the $Bi_3(NbTi)O_9$ phase is lower than that of the B_5N_3 phase. Since the 0.96B_5N_3-0.04B_4T_3 specimen showed an increased k value, the 0.96B_5N_3-0.04B_4T_3 films were deposited using PLD and their structural and electrical properties were investigated.

Figure 4(a) shows the SEM image of the 83 nm-thick 0.96B_5N_3-0.04B_4T_3 film grown at 300°C under an OP of 200 mTorr. This film was well developed with a sharp interface between it and the Pt electrode. An AFM image of the surface of this 0.96B_5N_3-0.04B_4T_3 film is shown in Fig. 4(b). The average roughness of the surface was approximately 0.7 nm, demonstrating its smoothness. Therefore, the 83 nm-thick, homogeneous 0.96B_5N_3-0.04B_4T_3 film was considered to be well formed on the Pt/Ti/SiO_2/Si substrate. Similar results were also observed in the other 0.96B_5N_3-0.04B_4T_3 films grown in this work.

Figure 5 shows the XRD patterns of the 0.96B_5N_3-0.04B_4T_3 films grown at various temperatures under 200 mTorr OP. For the films grown below 400°C, no peaks for the crystalline phase were observed, indicating the formation of the amorphous phase. However, even though no peak for the crystalline phase was observed in the specimens grown at 300 and 350°C, many small crystalline phases were thought to have formed in the film because a broad peak was found at approximately 28 degrees, as shown in the inset of Fig. 5 and many small crystalline phases were also found in the B_5N_3 film grown at 300°C.[17] Figure 5(c) shows the XRD patterns of the film grown at 400°C, in which the (111) peak for the B_3N crystalline phase was observed. The intensity of this peak considerably increased for the film grown at 500°C, as shown in Fig. 5(d), indicating that this film had a preferred growth orientation along the [111] direction. However, for the film grown at 600°C, the (200) peak of the B_3N phase was observed, indicating that this film has a random growth orientation. For the 0.96B_5N_3-0.04B_4T_3 ceramics fired at 1150°C, which is formation temperature of the PLD target, the B_5N_3 phase was a major phase and the B_3N phase was a low temperature phase of the B_5N_3. Therefore, the growth temperature (400 to 600°C) was not high enough to grow the film with a B_5N_3 phase, resulting in the formation

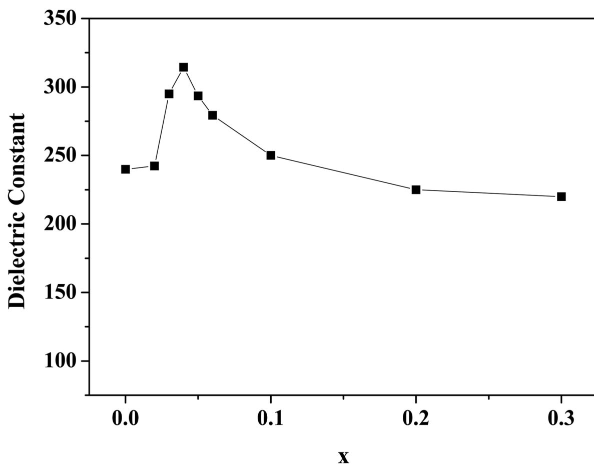

Fig. 3. Variation of the k values of the (1-x)B_5N_3-xB_4T_3 ceramics with $0.0 \leq x \leq 0.3$ sintered at 1150°C for 2 h.

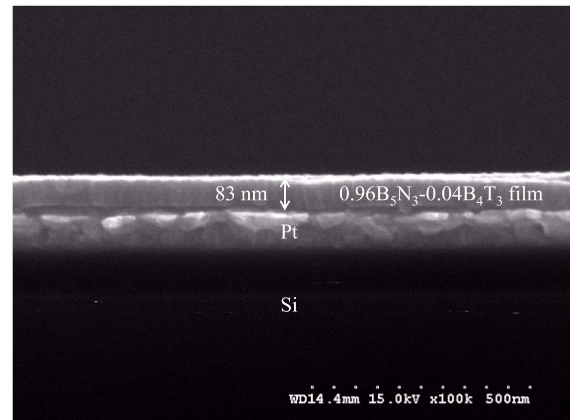

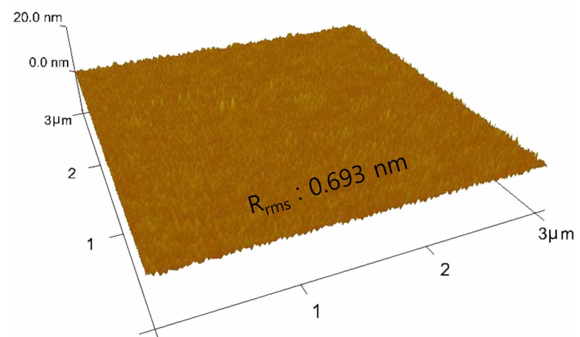

Fig. 4. (a) SEM and (b) AFM images of the 83 nm-thick 0.96B_5N_3-0.04B_4T_3 film grown at 300°C under an OP of 200 mTorr.

of B_3N phase.

The variation of the k value with growth temperature is shown in Fig. 6. The k value was already high at approximately 83 for the film grown at 300°C, probably due to the presence of the small crystalline phase and it increased to 92 for the film grown at 350°C, which was attributed to the increased number of small crystals. The k values of the films grown at 400 and 500°C were similar to that of the film grown at 350°C. The high k value of the film grown at 350°C implies that many small crystals were already formed in this film. The k value of the film grown at 500°C, which had a preferred growth direction along the [111] direction, was relatively low at approximately 91 and increased to 99 for the film grown at 600°C, which had a random growth orientation. Therefore, the dipole moment along the [111] direction of the B_3N phase was considered to be smaller than that of the random direction and a similar result was also observed in the B_5N_3 phase.[17]

Figure 7 show the variation of the leakage current density of the 0.96B_5N_3-0.04B_4T_3 film grown at 300°C under various OPs. The leakage current density was very high with a small breakdown field for the film grown under 100 mTorr OP but it considerably decreased for the film grown under 200 mTorr OP. For the films grown under low OPs, many oxygen vacancies were considered to have been formed and to have produced free electrons according to the following equation: $O_O = V_{OI}^{\bullet\bullet} + 2e' + \frac{1}{2}O_2$ where O_o is the oxygen ion on its normal site, $V_{OI}^{\bullet\bullet}$ the oxygen vacancy and e' the free electron. The number of oxygen vacancies decreased with increasing OP during the growth, thereby improving the electrical properties. However, the electrical properties of the films grown under the high OPs of > 200 mTorr were considerably degraded. In particular, the leakage current density of the film grown under an OP of 600 mTorr was high. Very few oxygen vacancies were considered to exist in the film grown under an OP of 200 mTorr because of its good electrical properties. Furthermore, it was considered that the oxygen interstitial ions (or metal vacancies) started to be formed in the films when the OP exceeded a certain critical value, presumed to be around 200 mTorr. The oxygen interstitial ions (or metal vacancies) produced the holes according to the following equation: $\frac{1}{2}O_2 = O_i'' + 2h^\bullet$ where O_i'' is an oxygen interstitial ion and $h^\bullet$ the hole. Therefore, the degradation of the electrical properties of the 0.96B_5N_3-0.04B_4T_3 films grown under high OPs of > 200 mTorr was attributed to the formation of the oxygen interstitial ions (or metal vacancies).

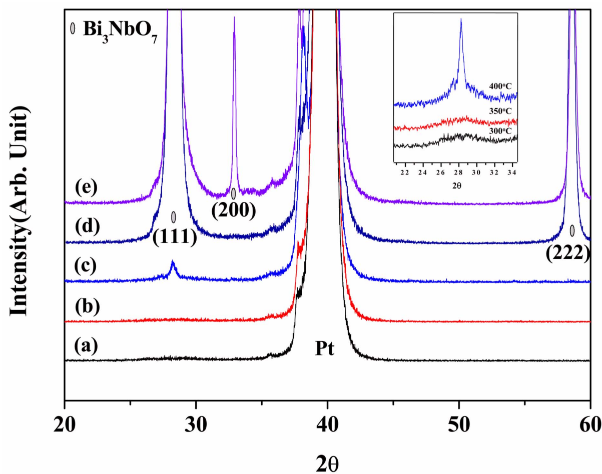

Fig. 5. XRD patterns of the 0.96B_5N_3-0.04B_4T_3 films grown at various temperatures under 200 mTorr OP: (a) 300°C, (b) 350°C, (c) 400°C, (d) 500°C, and (e) 600°C.

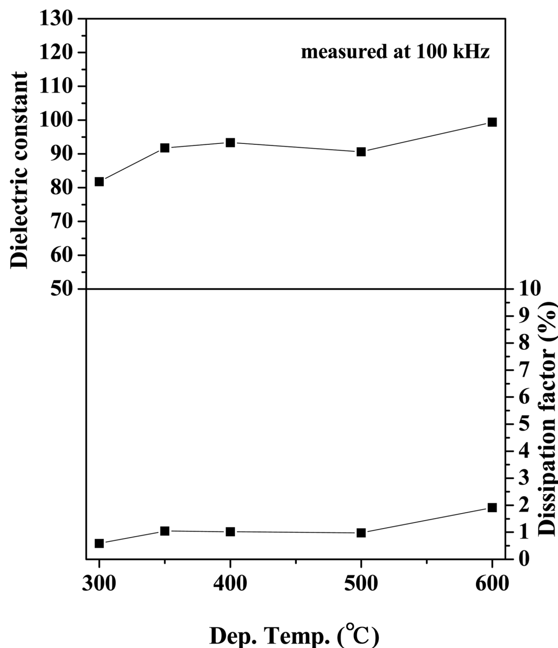

Fig. 6. Dielectric constant and dielectric loss of the 0.96B_5N_3-0.04B_4T_3 films grown at various temperatures.

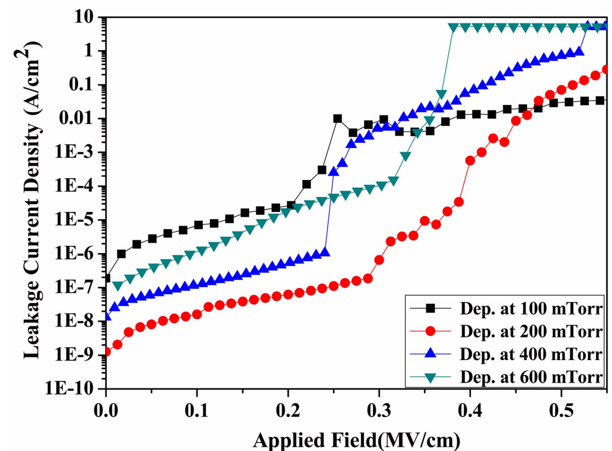

Fig. 7. Variation of the leakage current density of the 0.96B_5N_3-0.04B_4T_3 film grown at 300°C under various OPs.

4. CONCLUSION

The homogeneous B_5N_3 phase was formed in the (1-x)B_5N_3-xB_4T_3 ceramics with $0.0 \leq x \leq 0.03$ and both the B_5N_3 and $Bi_3(NbTi)O_9$ phases coexisted in the ceramics with $0.04 \leq x \leq 0.1$. The $Bi_3(NbTi)O_9$ phase was found when x exceeded 0.1. The k value of the ceramics considerably increased with the small addition of Ti, to a maximum value of 314 for the specimen with x = 0.04, probably due to the enhancement of the dipole moment by the replacement of the Nb^{5+} ions by Ti^{4+} ions. The 0.96B_5N_3-0.04B_4T_3 films were well formed on the Pt/Ti/SiO_2/Si substrate. For the films grown below 400°C, an amorphous phase was developed but the small B_3N crystals were considered to have been formed. The k value of the films grown at 300 °C was high at approximately 83, probably due to the presence of the small B_3N crystals. The leakage current density of the 0.96B_5N_3-0.04B_4T_3 film grown at 300°C under an OP of 100 mTorr was high with a small breakdown field due to the presence of the oxygen vacancies. As OP increased, the leakage current density decreased due to the decreased number of oxygen vacancies. However, as OP exceeded 200 mTorr, the electrical properties were degraded, probably due to the formation of oxygen interstitial ions. The 0.96B_5N_3-0.04B_4T_3 film grown at 300°C exhibited the high k value of 83 with a low dielectric loss of 0.5% and a low leakage current density of 8×10^{-8} A/cm^2 at 0.3 MV/cm with a high breakdown field of 0.4 MV/cm, indicating the suitability of this film as a candidate material for the capacitors that require a high k and low processing temperature.

ACKNOWLEDGMENT

This research was supported by a grant from the Fundamental R&D Program for Core Technology of Materials funded by the Ministry of Intelligence and Economy, Republic of Korea.

REFERENCES

1. *International Technology Roadmap for Semiconductors*, Semiconductor Industry Association, San Jose, CA (2005).
2. S. K. Bhattacharya and R. R. Tummala, *J. Mater. Sci.: Materials in Electronics* **11,** 253 (2000).
3. K. C. Chiang, C. C. Huang, A. Chin, W. J. Chen, S. P. McAlister, H. F. Chiu, J. R. Chen, and C. C. Chi, *IEEE Electr. Device Lett*. **26**, 504 (2005).
4. D. Brassard, L. Ouellet, and M. A. El Khakani, *IEEE Electr. Device Lett.* **28**, 261 (2007).
5. K. C. Chiang, C. C. Huang, G. L. Chen, W. J. Chen, H. L. Kao, Y.-H. Wu, A. Chin, and S. P. McAlister, *IEEE Trans. Electron Dev.* **53**, 2312 (2006).
6. Ch. Wenger, G. Lippert, R. Sorge, T. Schroeder, A. U. Mane, G. Lupina, J. Dabrowski, P. Zaumseil, X. Fan, L. Oberbeck, U. Schroeder, and H.-J. Mussig, *IEEE Trans. Electron Dev.* **53**, 1937 (2006).
7. C. D. Dimitrakopoulos, S. Purushothanman, J. Kymissis, A. Callegari, and J. M. Shaw, *Science* **283**, 822 (1999).
8. C. Bartic, H. Jansen, A. Campitelli, and S. Borghs, *Org. Electron*. **3**, 65 (2002).
9. L. A. Majewski, M. Grell, S. D. Ogier, and J. Veres, *Org. Electron*. **4**, 27 (2003).
10. T. Kim, A. I. Kingon, J. P. Maria, and R. T. Croswell, *J. Mater. Res.* **19**, 2841 (2004).
11. A. I. Kingon and S. Srinivasan, *Nature Materials* **4**, 233 (2005).
12. C. H. Choi, J. Y. Choi, K. H. Cho, M. J. Yoo, J. H. Choi, S. Nahm, C. Y. Kang, S. J. Yoon, and H. J. Lee, *J. Electrochem. Soc.* **155**, G87 (2008).
13. J. H. Park, W. S. Lee, N. J. Seong, S. G. Yoon, S. H. Son, H. M. Chung, J. S. Moon, H. J. Jin, S. E. Lee, J. W. Lee, H. D. Kang, Y. K. Chung, and Y. S. Oh, *Appl. Phys. Lett.* **88**, 192902 (2006).
14. I. D. Kim, M. H. Lim, K. T. Kang, H. G. Kim, and S. Y. Choi, *Appl. Phys. Lett.* **89**, 022905 (2006).
15. K. P. Hong, Y. H. Jeong, S. Nahm, C. Y. Kang, and S. J. Yoon, *IEEE Electr. Device Lett.* **29**, 334 (2008).
16. J.-H. Park, C.-J. Xian, N-J. Seong, S.-G. Yoon, S.-H. Son, H.-M. Chung, J.-S. Moon, H.-J. Jin, S.-E. Lee, J.-W. Lee, H.-D. Kang, Y.-K. Chung, and Y.-S. Oh, *Microelectron. Reliab.* **47**, 755 (2007) .
17. K.-H. Cho, C.-H. Choi, Y. H. Jeong, S. Nahm, C.-Y. Kang, S.-J. Yoon, and H.-J. Lee, *J. Electrochem. Soc.* **155**, G148 (2008).
18. K.-H. Cho, C.-H. Choi, K. P. Hong, J.-Y. Choi, Y. H. Jeong, S. Nahm, C.-Y. Kang, S.-J. Yoon, and H.-J. Lee, *IEEE Electr. Device Lett.* **29**, 684 (2008).
19. T. Takenaka, K. Komura, and K. Sakata, *Jpn. J. Appl. Phys.*, *Part 1*, **35**, 5080 (1996).